Increasing Photo-Fenton Process Efficiency: The Effect of Temperature

J. Carbajo*, J. E. Silveira, G. Pliego, J. A. Zazo, J.A. Casas

[a] Chemical Engineering Department, Universidad Autonoma de Madrid, 28049 Madrid, Spain

*Corresponding author. Tel: +34 914975599. E-mail address: jaime.carbajo@uam.es

Abstract

The possibility to intensify the homogeneous photo-Fenton by temperature (up to 90 ºC) has been deeply investigated employing phenol solutions as model pollutant and treating a real landfill leachate effluent.

TOC removal rate was significantly increased as temperature was raised in photo-oxidation experiments. Thus, 120 min of irradiation time was used to mineralize 1 g/L of phenol at 50 ºC, but only 30 min were needed to achieve the same result at 90 ºC. H_2O_2 consumption efficiency (η_{H2O2}), defined here as g of TOC converted per g of H_2O_2 consumed, increased from 0.085 at 25ºC to 0.144 at 50 ºC remaining unaffected up to 90 ºC. More interestingly, the Irradiation Energetic Efficiency, defined as the TOC converted per W-h of energy emitted to the solution, dramatically increased with temperature, and a maximum value of 1.04 g of TOC per W-h was reached at 90 ºC.

Similarly, when a much more complex wastewater matrix was evaluated, such as the landfill leachate, the required irradiation time to achieve maximum TOC and COD removals (around 80 %) was reduced from 180 to 45 min by increasing temperature from 50 to 90 ºC. Thus, irradiation efficiency increased 4-fold over the studied range of temperature.

In addition, a kinetic model was proposed to fit experimental data for TOC evolution in both phenol and the leachate treatment. According to this, firstly temperature promotes the rapid degradation of TOC by the hydroxyl radicals produced by Fenton reaction decreasing the wastewater turbidity and colour. Subsequently, photo-Fenton reaction plays a key role, promoting organic acids and other by-products mineralization.

The results of this paper reveal that, far from being a drawback due to undesirable H_2O_2 thermal decomposition into O_2 and H_2O, temperature could be efficiently used to enhance the cost-efficiency of photoassisted processes. To the best of our knowledge, this is the first time that such a wide range of temperature up to 90 ºC is explored. Thereby, new operational conditions to successfully treat moderate to highly organic loaded wastewaters are provided in this work.

Keywords: Photo-Fenton, Temperature Intensification, Irradiation Energetic Efficiency, leachate lixiviate treatment

1. Introduction

Advanced Oxidation Processes (AOPs) have been extensively applied to treat wastewater with toxic or non-biodegradable compounds [1-4]. Among them, Fenton process is based on the H_2O_2 catalytic decomposition by Fe^{2+} at acidic pH to produce active hydroxyl radicals ($HO^{\bullet}$) via Eq. 1. Fe^{2+} can be regenerated by H_2O_2 (see Eq. 2) or by interaction with organic compounds. Nevertheless, these reactions are several orders of magnitude slower than iron oxidation. Therefore, Fe^{2+} regeneration is considered the limiting step in the Fenton process [5].

$$Fe^{2+} + H_2O_2 \rightarrow Fe^{3+} + OH^- + HO^{\bullet} \quad \text{(Eq. 1)}$$

$$Fe^{3+} + H_2O_2 \rightarrow Fe^{2+} + HO_2^{\bullet} + H^+ \quad \text{(Eq. 2)}$$

There are several commercial wastewater treatment facilities based on Fenton technology, i.e. OHP® and MFC-Foret® processes [6,7]. These have proven to be efficient techniques to treat wastewaters with non-biodegradable pollutants. Both processes work at high temperature and use mixtures of iron salts.

The rate of Fenton reactions can be significantly increased by irradiating at wavelengths below to 580 nm in the so-called photo-Fenton process. This enhancement is mainly attributable to photoreduction of Fe^{3+}-ligand complexes, which dissociate into Fe^{2+} and oxidized ligand (LOH) through ligand-to-metal charge transfer (LMTC) mechanism [5,10]:

$$[Fe^{3+}L]\cdot H_2O + h\nu \rightarrow [Fe^{3+}L]^{*}\cdot H_2O \rightarrow Fe^{2+} + LOH + H^{+} \qquad \text{(Eq. 3)}$$

As a consequence, photoreduced Fe^{2+} can be subsequently re-oxidized by hydrogen peroxide producing hydroxyl radicals (see Eq. 1) [8,9], thus completing the catalytic cycle [5].

An interesting example of the previous photoreduction mechanism is the absorption of visible light between 500 and 580 nm by ferric-oxalate complexes (see Eqs. 4 and 5), which otherwise would be refractory to conventional Fenton process [10]:

$$Fe(C_2O_4)_3^{3-} + h\nu\ (\lambda<580\ nm) \rightarrow Fe^{2+} + 2\ C_2O_4^{2-} + C_2O_4^{-\bullet} \qquad \text{(Eq. 4)}$$

$$C_2O_4^{-\bullet} + Fe^{3+} \rightarrow Fe^{2+} + 2\ CO_2 \qquad \text{(Eq. 5)}$$

Despite these advantages, the industrial implementation of photo-Fenton process is still limited due to irradiation energy consumptions, Fenton reagent costs or low reaction rate when solar irradiation is employed [8,11]. Many strategies have been explored to increase photo-Fenton efficiency. Among them, the use of iron ligand complexes such as iron oxalate or iron citrate to avoid iron precipitation [12,13], or the integration of photo-

Fenton with other processes as ozone [14], photocatalysis with TiO_2 [15], nanofiltration [16], ultrasounds [17], biological or electrochemical processes [18-20].

Increasing temperature has been claimed to substantially enhance both, the oxidation rate and the mineralization degree in Fenton treatment processes [21-23]. Although increasing temperature is also considered to improve reaction rate in photo-Fenton [10], surprisingly, a very few number of works have study this effect beyond 50 ºC. This can be probably explained because it is generally accepted that at high temperature, photo-Fenton efficiency is compromised by H_2O_2 thermal decomposition into O_2 and H_2O [11] or iron hydroxide precipitation [8,24]. Moreover, the results gathered in literature seem to be divergent. Thus, Perez *et al.* [25] assessed the role of temperature, in the range 25-70 ºC, using wastewater from textile industry. According to their results, the higher the temperature, the higher the organic load removed. On the contrary, other authors reported the highest organic load conversion around 50ºC [26] or very scarce improvements beyond that temperature [27].

Therefore, this study tackles on the effect of temperature (between 25 and 90 ºC) upon photo-Fenton efficiency in terms of irradiated energy (W-h) and H_2O_2 consumption per TOC mineralized employing phenol as model pollutant. These results are ultimately validated by treating a much more complex matrix coming from a landfill leachate wastewater. Commonly, COD content in this latest effluent is related to the presence of significant amounts of high-weight recalcitrant compounds [28]. In this type of effluents, active oxidant species generated by photo-Fenton mechanism have turned into a promising alternative to conventional biological processes, particularly when the age of the leachates are above 5 years and BOD_5/COD ratios are below 0.2-0.3 [11].

Besides, a kinetic model based on two oxidation steps is proposed to accurately fit the TOC evolution throughout the oxidation by photo-Fenton process. An initial stage

dominated by hydroxyl radical formation from Fenton hydrogen peroxide decomposition and, a second one, in which photo-Fenton reactions allow short chain acids mineralization.

To the best of our knowledge, this is the first time that a such wide range of temperature up to 90 ºC is explored to analyze if photo-Fenton process can be enhanced by temperature to treat moderate to highly organic loaded wastewaters. Thus, reducing the accumulated UV-Vis energy requirements, employing low iron doses and minimizing $Fe(OH)_3$ sludge formation upon the oxidation process.

2. Materials and Methods

2.1. Chemicals

All the chemicals were analytical grade reagents and were used without further purification. Phenol (> 99%), H_2O_2 (33% w/w), $FeCl_2.4H_2O$ (> 99%), $TiOSO_4$, $AgSO_4$, $K_2Cr_2O_7$, Na_2CO_3 and $NaHCO_3$ were purchased from Sigma Aldrich, and HCl (37%) from Panreac. Working standard solutions of aromatics (p-benzoquinone, hydroquinone, catechol and resorcinol) and short-chain organic acids (fumaric, malonic, maleic, acetic and formic acids) from Sigma-Aldrich were prepared for calibration purposes.

2.2 Landfill leachate wastewater effluent

The leachate wastewater was obtained from a municipal landfill located in Madrid (Spain). The effluent was gravity filtrated before characterization and photo-Fenton oxidation experiments. The main parameters of the effluent are shown in Table 1. Nitrogen Content was around 750 mg/L, COD and TOC initial values were 2,930 and 891 mg/L, respectively. In addition, 1,125 mg/L of Cl^-, 280 mg/L of SO_4^{2-} and 431 mg/L

of Total Inorganic Carbon were also present, being the last attributable to the presence of HCO_3^- according to the slightly basic character (pH ~8.0) of the leachate.

2.3 Photo-Fenton experiments

Photo-Fenton experiments were carried out in an immersion-wall batch jacketed 1 L photoreactor equipped with a 150 W medium pressure Hg lamp (TQ-150 from Heraeus) contained in a water-cooled quartz chamber provided with a temperature control unit Ministat 125 (Huber). The photoreactor was placed in a heating plate to accurately control the temperature in the reaction media ensuring minimal deviation ($\pm$1 ºC). The lamp emits in a broad spectrum between 250 and 600 nm, with a UV-irradiance of 30 $W \cdot m^{-2}$. Photo-Fenton experiments were carried out as follows: briefly, 600 mL of a pH_0 3 phenol aqueous solution or landfill leachate wastewater containing the required amount of Fe^{2+} catalyst (10 mg/L) were premixed in the reactor. Afterwards the solution was heated up to the desired temperature. Finally, the stoichiometric amount of H_2O_2 required to complete TOC mineralization was added and the lamp irradiation was turn on, being this step the beginning of the reaction. Hereafter, liquid aliquots were sampled from the reactor at different time intervals, immediately cooled at 5 ºC and subsequently analysed by HPLC, ionic chromatography and Total Organic Carbon. Temperature was varied within 25-90 ºC. For the sake of comparison, Fenton experiments were carried out at the same operating conditions in absence of irradiation.

2.4 Analytical methods

Phenol and aromatic by-products were analyzed and quantified by high performance liquid chromatography (Thermo Fisher Scientific) using a C18 column (Eclipse Plus C18, 150 x 4.6 mm, 5 μm) at 323 K with a 4 mM aqueous sulfuric acid solution at 1 $mL \cdot min^{-1}$ as mobile phase. Short-chain organic acids and other inorganic anions were analyzed by ion chromatography (IC) equipped with a conductivity detector (Metrohm 883 IC) using

a Metrosep A supp 5 column (250 x 4 mm) and 0.7 mL·min^{-1} of an aqueous solution of 3.2 mM Na_2CO_3 and 1 mM $NaHCO_3$ as the mobile phase. Total organic carbon (TOC), Total Inorganic Carbon (IC) and Total Nitrogen (TN) in solution were measured using a TOC analyzer (Shimadzu, mod. TOC-Vsch and TOC-L). H_2O_2 concentration was determined by colorimetric $TiOSO_4$ method using a UV2100 Shimadzu UV–vis spectrophotometer.

The Chemical Oxygen Demand (COD) measurements were performed by colorimetric method using a UV−vis spectrophotometer (Shimadzu, model. UV-1603) in accordance with a standard method using potassium dichromate as oxidant (ISO 6060).

3. Results and discussion

3.1 Influence of temperature on photo-Fenton performance with phenol

Figure 1 illustrates the evolution of Total Organic Carbon (TOC) and H_2O_2 concentrations upon the photo-Fenton oxidation of 1000 mg/L of phenol at different temperatures employing 10 mg/L of Fe^{2+} and the stoichiometric amount of hydrogen peroxide. For the sake of comparison, the experimental data carried out in absence of light (dark Fenton process) are also included.

It must be noted that the Fe/H_2O_2 ratio is significantly lower than the regular used for Fenton process [29], in an attempt to minimize the effect of iron dose upon the kinetic, thus making more noticeable the effect of temperature. Moreover, the sludge generation and the scavenger reactions among H_2O_2 and/or hydroxyl radicals are also minimized [22].

As can be observed in Figure 1, the increases of temperature promote a higher rate of H_2O_2 decomposition and, consequently, higher TOC conversion. Thus, while 120 min of irradiation time are required to degrade 95 % of TOC at 50 ºC, only 30 min were needed

to achieve the same degree of mineralization at 90 ºC. In terms of H_2O_2 efficiency (η_{H2O2}), defined here as the g of TOC removed per g of hydrogen peroxide consumed, this value changed from 0.085 at 25ºC to 0.144 at 50 ºC (see Table 2). Beyond this temperature, the efficiency was maintained up to 90 ºC. The maximum value of this efficiency would be 0.152 considering only TOC conversion.

On the basis of these results, it can be clearly stated that the increase of temperature in photo-Fenton process, far from being a drawback due to undesirable H_2O_2 thermal decomposition, increase TOC rate removals and H_2O_2 consumption efficiencies.

Figure 2 depicts the evolution of oxidation intermediates, including aromatics (phenol, hydroquinone, p-benzoquinone and catechol) and short-chain organic acids (malonic, maleic, formic and oxalic) along the reaction at different temperatures. In addition, the differences between the measured TOC values and the amount of carbon in the identified compounds (i.e. short chain acids and aromatic compounds) has been defined as unidentified TOC, which may be attributed in a certain extent to condensation by-products [30,31] and other unknown oxidation intermediates. As can be seen, phenol and aromatics were not completely removed at temperatures below 50 ºC, and the subsequent evolution of short-chain organic acids and other by-products was limited by the extent of phenol-aromatic oxidation. This was particularly true at 25 ºC, where an intense brown colour in the solution was observed. This coloration, mainly attributable to the appearance of quinones and condensation by-products, prevented photochemical reactions inside the photoreactor.

At higher temperatures (above 50 ºC), although a less intense brown colour was also observed, it rapidly disappeared. Therefore, temperature appears to promote oxidation of phenol and aromatic by-products to acids. Despite these acids are poorly reactive with

hydroxyl radicals, they are prone to be easily removable trough photodecomposition reactions in which iron salts are involved. In this sense, as can be seen in Figure S1 (Supporting Information), oxalic acid degradation was significantly accelerated as the temperature increased, achieving complete degradation even at 50 ºC. Conversely, oxalate ferric degradation appears to be the rate-limiting step in the dark Fenton experiments even at 90 ºC (see Fig. S1).

The effect of the temperature on the H_2O_2 consumption efficiency is also corroborated by the results shown in Figure 3, which depicts the X_{TOC} *vs.* X_{H2O2} for all the photo-Fenton experiments at different times and temperatures. For the sake of comparison, it also includes the results obtained in dark conditions at 90 °C after 240 min of reaction time. As can be seen, the ratio TOC converted *v*s. H_2O_2 consumed did not decreased as increasing temperature, as should occurs if H_2O_2 would predominantly decomposed into O_2 and H_2O. On the contrary, in those photo-Fenton experiments performed at or above 50 ºC, X_{TOC}/X_{H2O2} ratios increased to values that are close to the unit. At this conditions, when temperature is high enough, effluent turbidity is rapidly reduced and Fe-organic complexes may be broken by photolysis (see Eqs. 4 and 5) reducing Fe^{3+} to Fe^{2+} (see Eq. 3). By contrast, when temperature was below 50 ºC, photo-Fenton reactions were severely limited by the inability of light to penetrate in the wastewater and X_{TOC}/X_{H2O} ratio was lower than 0.8 (see Figure 3).

Unlike other conventional process, the cost of irradiation is an important factor limiting the industrial application of photo-Fenton processes [8]. In this sense, high illuminated surface to volume ratios are needed to achieve good efficiencies in solar photo-reactors, thereby capital and operational costs associated to scaling-up and high surface requirements are increased. On the other hand, the operating costs associated to energy consumption can severely increase when artificial lamps are employed as a source of

irradiation. Whichever the case may be, it can be easily understand the relevance of the energetic efficiency of irradiation from an industrial perspective to analyze the photo-Fenton cost-efficiency. To this aim, herein we have defined the "Irradiation Energetic Efficiency" (IEE) [32] as the amount of organic carbon mineralized per W-h of energy emitted to the solution. Accordingly, the energy accumulated (Q_{UV}) in W-h for all the irradiated experiments has been calculated as peer Eq. 6:

$$Q_{UV} = UV_G \cdot A_i \cdot \Delta t_n \quad \text{(Eq. 6)}$$

where UV_G is the emitted lamp UV-irradiance (30 W·m^{-2}), A_i is the irradiated area and t_n the experimental reaction time. The corresponding Irradiation Energetic Efficiencies (IEE), has been accordingly represented in Table 2. As can be seen, IEE values severely increase with temperature, achieving a maximum value of 1.04 g of TOC removed per W-h at 90 ºC, otherwise only 0.26 g of TOC could be degraded at 50 ºC employing the same amount of energy. It should be noted that IEE parameter does not provide information about the efficiency of the photocatalytic reactor design or about the rate at which molecules undergo a given oxidation event per photon absorbed (quantum yield) [32]. Nonetheless, IEE undoubtedly better illustrates the impact of the TOC disappearance rate on the economic viability of the photo-Fenton process from an industrial applicability perspective.

3.2 Influence of temperature on the photo-Fenton process kinetic model

To more deeply analyze the effect of temperature on the photo-Fenton process and to get valuable data for design purposes, a kinetic model to fit the experimental data has been proposed. In this sense, the evolution of TOC under different temperatures (see Figure 2) strongly suggests that in an initial phase the oxidation process is dominated by the Fenton reaction. Then, TOC curves change their trend indicating the point at which the photo-

Fenton reactions becomes dominant. Accordingly, a kinetic model previously reported for Fenton oxidation [21] has been re-designed to fit photo-Fenton experiments. Two types of TOC have been defined to better fit the experimental data as illustrated in Scheme 1. TOC_A can been ascribed to phenol, aromatics or other oxidation intermediates such as condensation by-products which can be easily oxidized by hydroxyl radicals to CO_2 (k_1) or other oxygenated by-products TOC_B (k_2). TOC_B is composed of short-chain organic acids and other unidentified TOC which can be photo-oxidized to CO_2 (k_3). For this model, an apparent second order has been proposed to fit TOC_A disappearance rate, typically describing Fenton processes [21,33] while, in accordance with experimental data, TOC_B mineralization to CO_2 has been fitted to a zero apparent kinetic order, describing accurately the photo-oxidation reactions:

$$TOC = TOC_A + TOC_B \quad \text{(Eq. 7)}$$

$$\frac{\partial TOC_A}{\partial t} = -k_1 \cdot TOC_A^2 - k_2 \cdot TOC_A^2 \quad \text{(Eq. 8)}$$

$$\frac{\partial TOC_B}{\partial t} = k_2 \cdot TOC_A^2 - k_3 TOC_B{}^0 \quad \text{(Eq. 9)}$$

The corresponding calculated apparent kinetic constants are represented in Table 3, while the corresponding fit to experimental TOC values is depicted in Figure 4. All rate constants were obtained by fitting the model to the experimental data using Scientist 3.0 software. The goodness-of-fit of the data to the curves is certainly corroborated by Figure 5, where the simulated TOC *vs.* experimental TOC is represented.

As can be seen in Table 3, all the apparent rate constants within the range 25-90 ºC significantly increase with temperature. Interestingly, these results confirm that the oxidation process is enhanced by temperature in a first stage through the intensification of $HO^{\bullet}$ formation by conventional Fenton, promoting faster aromatics oxidation and condensation by-products to acids (k_2) and direct oxidation of TOC_A to CO_2 (k_1). The later may be related to the release of CO_2 during the initial oxidative ring opening of the

aromatic intermediates accordingly to previous studies [31,33]. Once the turbidity is significantly reduced, photo-Fenton reactions dominate the oxidation process and TOC_B mineralization is accelerated trough photodecomposition reactions by iron species occurring all over the reactor depth, being this confirmed by the dramatic increase of k_3 values with temperature.

3.3 Influence of temperature on the landfill leachate wastewater treatment by photo-Fenton

The possibility to increase photo-Fenton efficiencies at high temperature has been ultimately tested by treating a much more complex wastewater, as the landfill leachate effluent selected for this work (characteristics are provided in Table 1).

Experiments were carried out at 50 and 90 ºC employing 10 mg/L of Fe^{2+} following the same conditions of the study conducted with phenol in previous sections. H_2O_2 initial concentration was the theoretical amount required to completely remove the initial COD (1g COD <> 2.125 g H_2O_2 [34]), and pH was adjusted to 3 prior to the reaction. Thus, $CO_3^{\bullet-}$ formation via $HO^{\bullet}$ scavenging by carbonate anions was avoided [35].

As can be seen in Figure 6, as occurred with phenol, increasing temperature from 50 to 90 ºC dramatically decreased the required irradiation time (from 180 to 45 min) to achieve the maximum TOC removal (around 80 %), being the remaining TOC consistently explained by H_2O_2 depletion. Even more interestingly, the Irradiation Energetic Efficiency (IEE) increased by 4 fold with temperature (see Table 4). Thus while 0.68 g of TOC were eliminated per W-h at 90 ºC, uniquely 0.17 g of TOC could be degraded at 50 ºC employing the same amount of energy. It is also noticeable how hydrogen peroxide efficiency (η_{H2O2}), represented in Table 4, were roughly equal at 50 and 90ºC, proving that the undesirable H_2O_2 thermal decomposition into O_2 and H_2O was not significant at high temperatures.

Based on the kinetic model proposed in the previous section (see Scheme 1), TOC experimental values for the landfill leachate photo-Fenton experiments at 50 and 90 ºC were also fitted. According to the apparent kinetic constants r^2 coefficients (see Table 5) and the corresponding fit to experimental TOC values, depicted in Figure 7, it can be confirmed that the proposed kinetic model is valid not only for phenol solutions as model pollutant, but to fit a much more complex effluent such as the leachate studied here. Also the role of temperature was confirmed by the increase of apparent kinetic constants. Thus, values for k_1, k_2 and k_3 for the experiment at 90 ºC were one order of magnitude higher than those obtained at 50 ºC.

Besides, although slightly differences were found when phenol solutions and leachate experiments were compared at 50 and 90 ºC, interestingly, k_1, k_2, and k_3 were found to be in the same order of magnitude. Accordingly, it may be postulated that, as occurs with phenol, in a first phase hydroxyl radicals produced by Fenton reaction are intensified by temperature inducing the fast oxidation of high-weight recalcitrant and the aromatic compounds present in landfill leachates wastewaters [28], resulting in a significant reduction of the effluent turbidity (see colour evolution in Figure S2). Subsequently, in a second phase, photo-Fenton reaction becomes dominant and photochemical reactions are promoted all over the reactor depth accelerating the mineralization organic acids and other dissolve organic matter present in landfill lixiviates such as alcohols or aldehydes [36].

4. Conclusion

Herein, the intensification of the photo-Fenton process by increasing temperature up to 90 ºC has been proposed to improve the mineralization efficiency for phenol solutions and a real landfill leachate effluent. The results reveal that, far from being a drawback

due to undesirable H_2O_2 thermal decomposition into O_2 and H_2O, temperature increase has led to high H_2O_2 consumption efficiencies. Meanwhile, the required amount of irradiated energy to degrade the organic matter is dramatically reduced with temperature in photo-Fenton oxidation. Thus, for phenol solutions and the landfill leachate, a maximum of 1.04 g and 0.68 g of TOC were eliminated per W-h at 90 ºC, respectively.

The TOC evolution upon the leachate and phenol oxidation has been satisfactorily fitted by a kinetic model considering two TOC fractions. The values of the apparent kinetic constants suggest that, in a first phase, temperature significantly intensifies $HO^{\bullet}$ formation by conventional Fenton pathway, promoting fast oxidation of aromatics and other by-products to acids and CO_2. Consequently, wastewater colour-turbidity was significantly reduced. In a second phase, dominated by photo-Fenton reactions, organics acids and other by-products removal is accelerated with temperature trough photochemical oxidation reactions occurring all over the reactor depth.

The present work provide new data indicating that relatively high temperatures up to 90 ºC can be efficiently applied in photo-Fenton processes to treat moderate to highly organic loaded real wastewaters. It should be remarked that, along with low irradiation energetic requirements, low operational costs might be maintained if wastewater is heated by sun light in low concentration photo-reactors. At the same time, kinetic improvement by temperature can reduce iron doses requirements, minimizing $Fe(OH)_3$ sludge formation upon the oxidation process.

Acknowledgments

This work has been supported by the following project: P2018/EMT-4341 (Consejería de Educación y Ciencia de la Comunidad Autónoma de Madrid). J. Carbajo wants to thank

the Ministerio de Ciencia, Innovación y Universidades (MICIU) for a grant under the Juan de la Cierva_Incorporación programme (IJCI-2017-32682).

References

[1] A. R. Ribeiro, O.C. Nunes, M.F.R. Pereira, A.M.T. Silva, Environ. Int. 75 (2015) 33

[2] I. Oller, S. Malato, J.A. Sánchez-Pérez, Sci. Total. Environ. 409 (2011) 4141

[3] J. Carbajo, A. Bahamonde, M. Faraldos, Mol. Catal. 434 (2017) 167

[4] C. Amor, L. Marchão, M. S. Lucas, J. A. Peres, Water 11 (2019) 205

[5] J. J. Pignatello, E. Oliveros, A. Mackay, Crit. Rev. Env. Sci. Tec. 36 (2006) 1

[6] M. Munoz, P. Domínguez, Z. M. de Pedro, J. A. Casas, J. J. Rodriguez, Appl. Catal. B: Environ. 203 (2017) 166

[7] N. Inchaurrondo, A. Maestre, G. Žerjav, A. Pintar, C. Ramos, P. Haure, J. Environ. Chem. Eng. 6 (2018) 2027

[8] D. Spasiano, R. Marotta, S. Malato, P. Fernandez-Ibáñez, I. Di Somma, Appl. Catal. B: Environ. 170-171 (2015) 90

[9] A. G. Gutierrez-Mata, S. Velázquez-Martínez, Alberto Álvarez-Gallegos, M. Ahmadi, J. A. Hernández-Pérez, F. Ghanbari, S. Silva-Martínez, Int. J. Photoenergy vol. 2017, Article ID 8528063, 27 pages, 2017. https://doi.org/10.1155/2017/8528063

[10] S. Malato, P.Fernández-Ibáñez, M.I. Maldonado, J. Blanco, W.Gernjak, Catal. Today 147 (2009) 1

[11] S. R. Pouran, A. R. Abdul Aziz, W. M. A. Wan Daud. J. Ind. Eng. Chem. 21 (2015) 53

[12] F. C. Moreira, J. Soler, A. Fonseca, I. Saraiva, R. A. R. Boaventura, E. Brillas, V. J.P.Vilar. Appl. Catal. B: Environ.182, (2016) 161

[13] D. R. Manenti, P. A. Soares, A. N. Módenes, F. R. Espinoza-Quiñones, R. A. R. Boaventura, R. Bergamasco, V. J. P. Vilar, Chem. Eng. J., 266, (2015) 203.

[14] J. Beltrán-Heredia, J. Torregrosa, J.R. Domínguez, J.A. Peres, Chemosphere 42

(2001) 351.

[15] J. Marugán, M.J. Lopez-Muñoz, W. Gernjak, S. Malato, Ind. Eng. Chem. Res. 45

(2006) 8900

[16] S. Miralles-Cuevas, I. Oller, A. Ruiz Aguirre, J. A. Sánchez Pérez, S. Malato Rodriguez, Chem. Eng. J. 239 (2014) 68

[17] R.A. Torres, J.I. Nieto, E. Combet, C. Pétrier, C. Pulgarin, Appl. Catal. B: Environ. 80 (2008) 168.

[18] M. M. Ballesteros Martín, J. A. Sánchez Pérez, J. L. García Sánchez, J. L. Casas López, S. Malato Rodríguez, Water Res., 43 (2009) 3838.

[19] A. Wang, J. Qu, H. Liu, J. Ru, Appl. Catal. B: Environ. 84 (2008) 393.

[20] A. Serra, X. Domènech, E. Brillas, J. Peral, J. Environ. Monit.,, 13 (2011) 167

[21] J. A. Zazo, G. Pliego, S. Blasco, J. A. Casas, J. J. Rodríguez, Ind. Eng. Chem. Res. 50 (2011) 866

[22] G. Pliego, J. A. Zazo, S. Blasco, J.A. Casas, J. J. Rodriguez, Ind. Eng. Chem. Res. 51 (2012) 2888

[23] G. Pliego, J. A. Zazo, J.A. Casas, J. J. Rodriguez,, J. Hazard. Mat. 252-253 (2013) 180

[24] A. Zapata, I. Oller, E. Bizani, J.A. Sánchez-Pérez, M. I. Maldonado, S. Malato, Catal. Today 144 (2009) 94

[25] M. Pérez, F. Torrades, X. Domènech, J. Peral, Water Res. 36 (2002) 2703

[26] F. Torrades, M. Perez, H. D. Mansilla, J. Peral, Chemosphere 53 (2003) 1211

[27] G. Sagawe, A. Lehnard, M. L¸bber, .D. Bahnemann, Hevetica chimica acta 84 (2001) 3742

[28] E. M. R. Rocha, F. S. Mota, V. J. P. Vilar, R. A. R. Boaventura

Environ. Sci. Pollut. Res. 20 (2013) 5994.

[29] V. Razaviarani, J. A. Zazo, J. A. Casas, P. R. Jaffé, Chemosphere

224 (2019) 653

[30] I. Magario, F.S. García Einschlag, E.H. Rueda, J. Zygadlo, M.L. Ferreira

J. Mol. Catal. A: Chem., 352 (2012) 1

[31] J. Carbajo, A. Quintanilla, J. A. Casa, Appl. Catal. B: Environ. 232 (2018) 55

[32] N. Serpone, J. Photochem. Photobiol. A: Chem.104 (1997) 1

[33] J. Carbajo, A. Quintanilla, A. L. Garcia-Costa, J. González-Julián, M. Belmonte, P. Miranzo, M.I. Osendi, J.A. Casas, Catal. Today Catalysis Today, https://doi.org/10.1016/j.cattod.2019.12.020

[34] M. S. Lucas, J. A. Peres. J. Hazard. Mater. 168 (2009), 1253.

[35] S.Yan, Y. Liu, L. Lian, R. Lia, J. Ma, H. Zhou, W. Song, Water Res.

161 (2019) 288

[36] O. Primo, M.J. Rivero, I. Ortiz, J. Hazard. Mat. 153 (2008) 834.

Table 1. Landfill leachate main parameters

Parameters	**Values**
COD, $mg \cdot L^{-1}$	2,930
TOC, $mg \cdot L^{-1}$	891
TN, $mg \cdot L^{-1}$	750
Inorganic Carbon-, $mg \cdot L^{-1}$	431
pH	7.9-8.1
Chloride, $mg \cdot L^{-1}$	1,125
Sulfate, $mg \cdot L^{-1}$	280
Conductivity, $mS \cdot cm^{-1}$	4.6

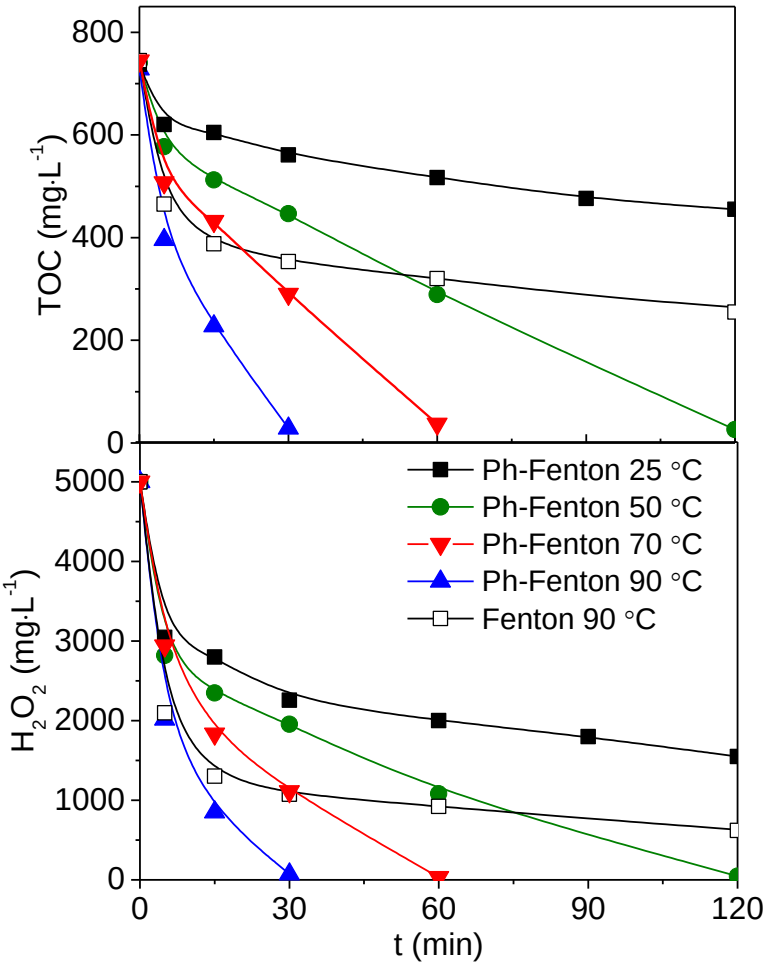

Figure 1. Effect of temperature on TOC and H_2O_2 concentration upon photo-Fenton (Ph-Fenton) and Fenton phenol oxidation.

($[Phenol]_0$=1000 mg/L, $[H_2O_2]_0$=5000 mg/L, $[Fe^{2+}]_0$ = 10 mg/L, pH_0 = 3)

Table 2. Hydrogen peroxide efficiency (η_{H2O2}) and Irradiation Energetic Efficiency (IEE) for photo-Fenton phenol oxidation runs at different temperatures

	η_{H2O2}[a]	IEE[b]
Photo-Fenton 25ºC	0.085	0.13
Photo-Fenton 50ºC	0.144	0.26
Photo-Fenton 70ºC	0.146	0.54
Photo-Fenton 90ºC	0.141	1.04
Fenton 90ºC	0.118	-

[a] gTOC removed/gH_2O_2 consumed

[b] gTOC removed per W-h at the maximum X_{TOC}

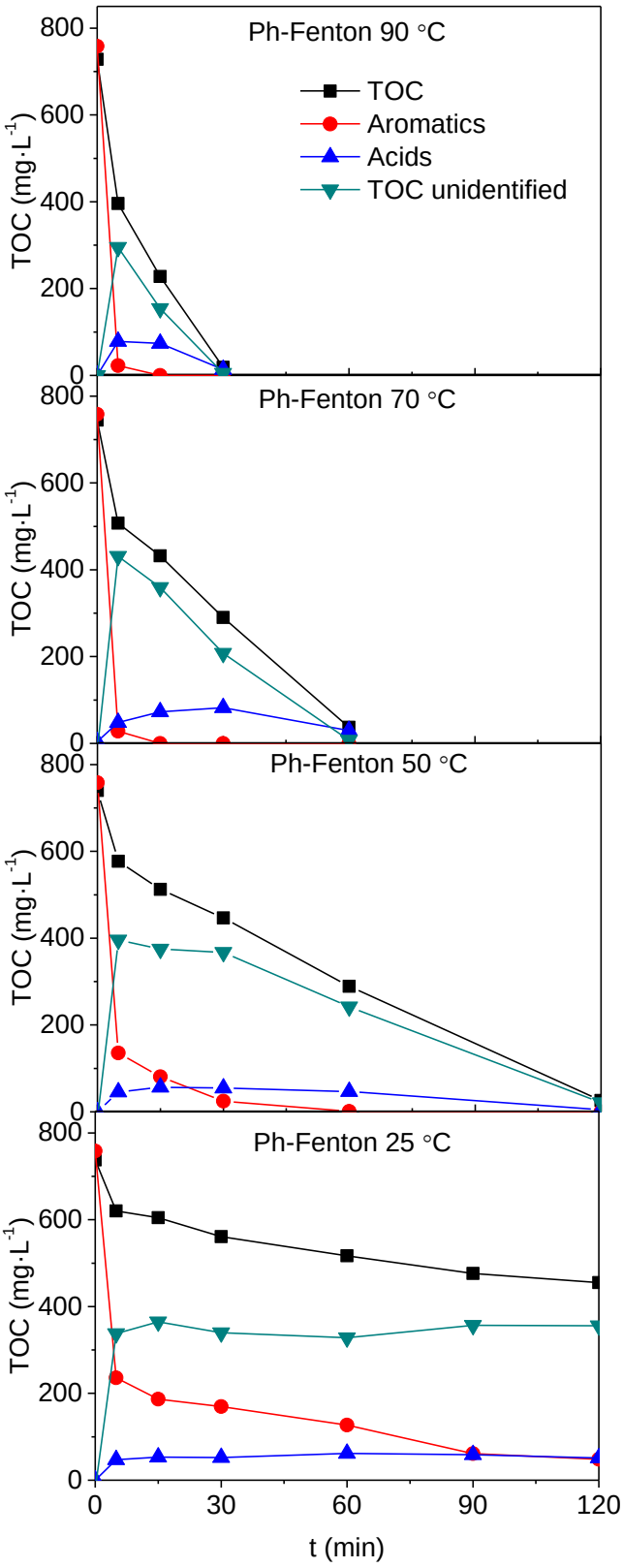

Figure 2. Evolution of TOC and oxidation by-products on the photo-Fenton phenol oxidation at different temperatures.

Operating conditions: ([Phenol]$_0$=1000 mg/L, [H_2O_2]$_0$=5000 mg/L, [Fe^{2+}]$_0$=10 mg/L, pH_0=3)

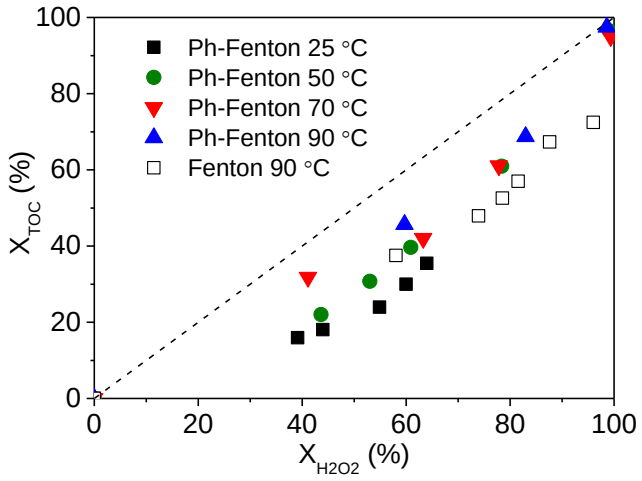

Figure 3. TOC *vs.* H_2O_2 conversions on the Fenton and photo-Fenton (Ph-Fenton) phenol oxidation at different temperatures.

Operating conditions: ([Phenol]$_0$=1000 mg/L, [H_2O_2]$_0$=5000 mg/L, [Fe^{2+}]$_0$=10 mg/L, pH_0= 3)

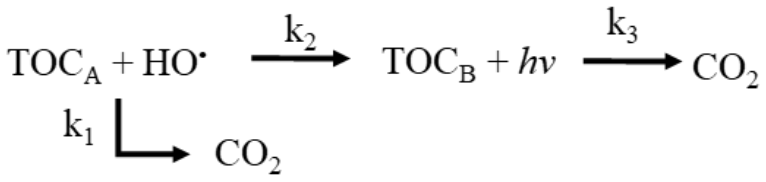

Scheme 1. Kinetic pathway

Table 3. Apparent kinetic rate constants on photo-Fenton phenol oxidation

k_1,k_2: L·mg^{-1}·min^{-1} ; k_3: mg·L^{-1}·min^{-1}

	k_1	k_2	k_3	r^2
25ºC	$8.91 \cdot 10^{-5}$	$2.98 \cdot 10^{-4}$	0.88	0.9997
50ºC	$1.74 \cdot 10^{-4}$	$5.20 \cdot 10^{-3}$	4.49	0.9998
70ºC	$6.81 \cdot 10^{-3}$	$1.97 \cdot 10^{-2}$	8.57	0.9998
90ºC	$1.18 \cdot 10^{-2}$	$1.93 \cdot 10^{-2}$	14.40	0.9994

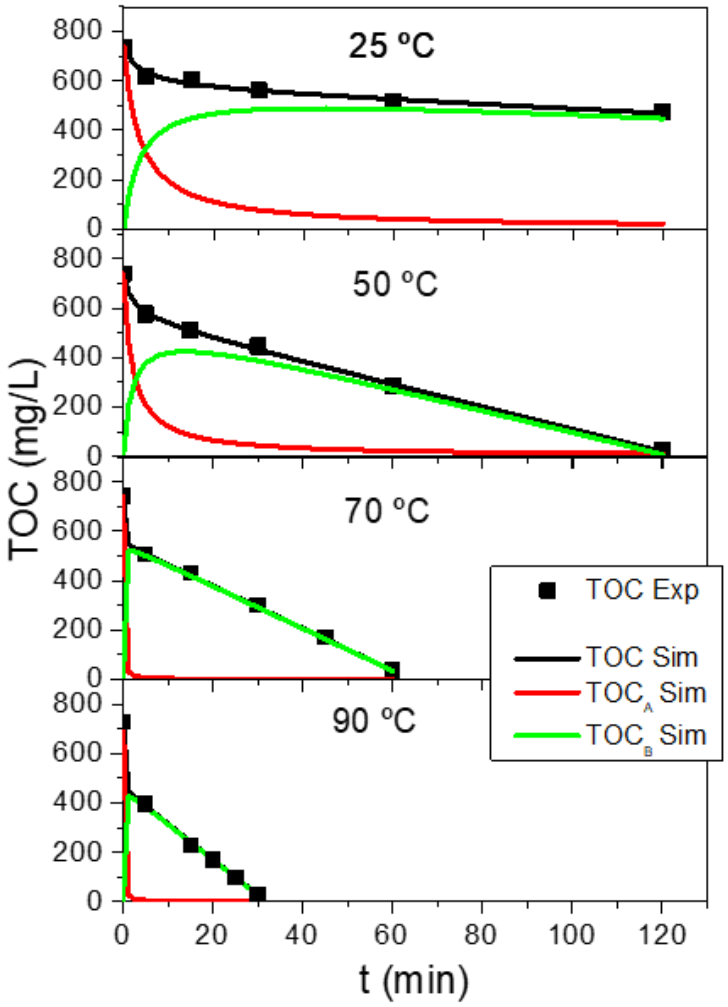

Figure 4. Experimental (symbols) and simulated (lines) TOC in Photo-Fenton phenol oxidation at different temperatures.

([Phenol]$_0$=1000 mg/L, [H_2O_2]$_0$=5000 mg/L, [Fe^{2+}]$_0$=10 mg/L, pH$_0$=3)

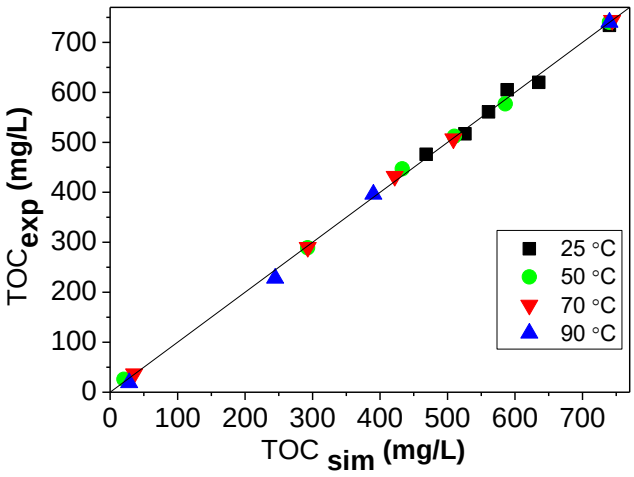

Figure 5. TOC parity plot

([Phenol]$_0$=1000 mg/L, [H_2O_2]$_0$=5000 mg/L, [Fe^{2+}]$_0$=10 mg/L, pH_0 = 3)

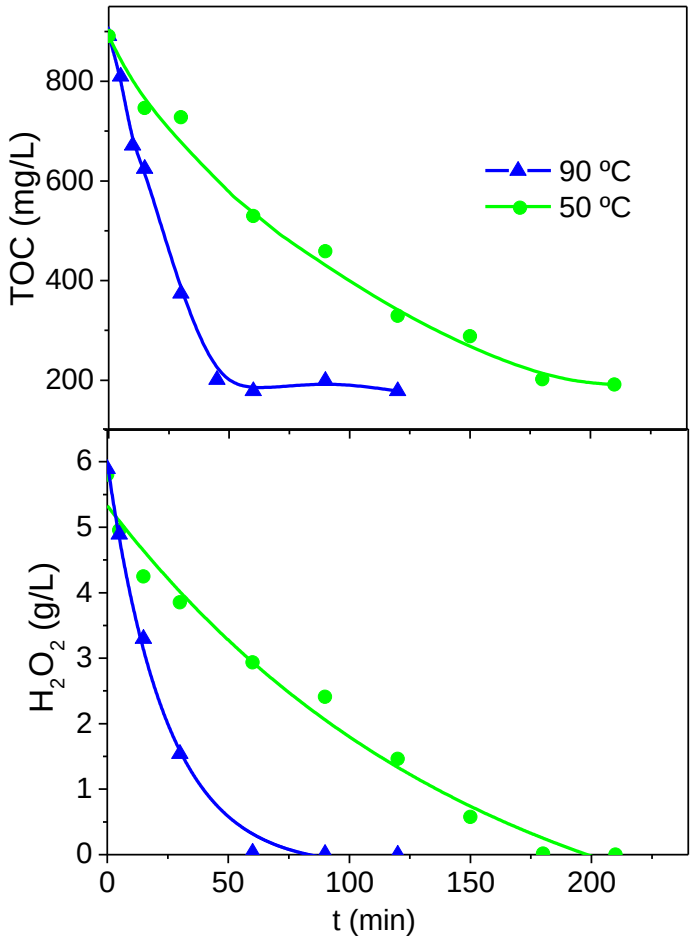

Figure 6. Effect of temperature on TOC and H_2O_2 concentration upon photo-Fenton landfill leachate wastewater treatment at different temperatures.

($[TOC]_0$=981 mg/L, $[DQO]_0$=2,930 $[H_2O_2]_0$=6200 mg/L, $[Fe^{2+}]_0$ = 10 mg/L, pH_0 = 3)

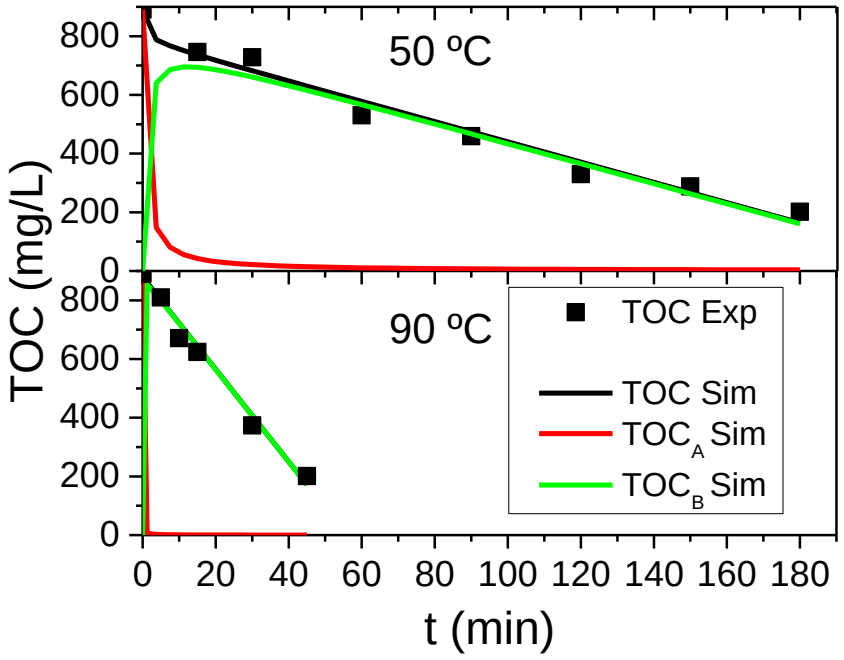

Figure 7. Experimental (symbols) and simulated (lines) TOC in Photo-Fenton landfill leachate wastewater treatment at different temperatures.

($[TOC]_0$=981 mg/L, $[DQO]_0$=2,930 $[H_2O_2]_0$=6200 mg/L, $[Fe^{2+}]_0$ = 10 mg/L, pH_0 = 3)

Table 4. Hydrogen peroxide efficiency (η_{H2O2}) and Irradiation Energetic Efficiency (IEE) for the Landfill Leachate photo-Fenton oxidation at different temperatures

	η_{H2O2}[a]	IEE[b]
PhotoFenton 50ºC	0.111	0.17
PhotoFenton 90ºC	0.112	0.68

[a] gTOC removed/gH_2O_2 consumed
[b] gTOC removed per W-h·L^{-1} consumed at the maximum X_{TOC}

Table 5. Apparent kinetic rate constants for Landfill Leachate photo-Fenton oxidation

	k_1,k_2: L·mg^{-1}·min^{-1} ; k_3: mg·L^{-1}·min^{-1}			
	k_1	**k_2**	**k_3**	**r^2**
50ºC	$1.82 \cdot 10^{-4}$	$1.32 \cdot 10^{-3}$	3.40	0.997
90ºC	$1.41 \cdot 10^{-3}$	$1.07 \cdot 10^{-2}$	15.73	0.997

Increasing Photo-Fenton Process Efficiency: The Effect of Temperature

J. Carbajo*, J. E. Silveira, G. Pliego, J. A. Zazo, J.A. Casas

[a] Chemical Engineering Department, Universidad Autonoma de Madrid, 28049 Madrid, Spain

*Corresponding author. Tel: +34 914975599. E-mail address: jaime.carbajo@uam.es

Supporting Information

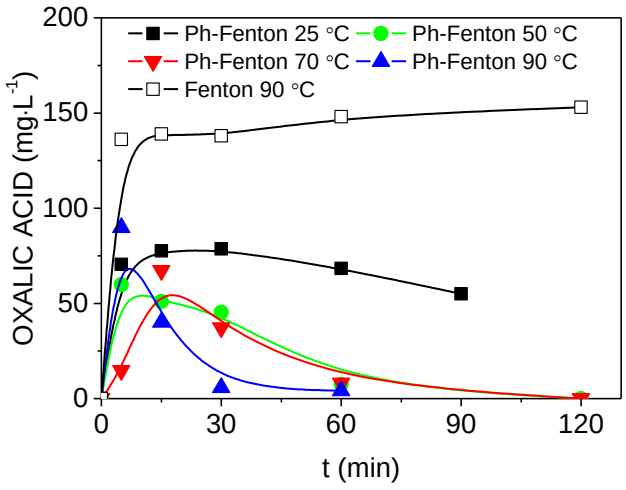

Figure S1. Oxalic acid evolution on the photo-Fenton (Ph-Fenton) and Fenton phenol oxidation at different temperatures.

Operating conditions: ($[Phenol]_0$=1000 mg/L, $[H_2O_2]_0$=5000 mg/L, $[Fe^{2+}]_0$ = 10 mg/L, pH_0 = 3, T=25-90 ºC)

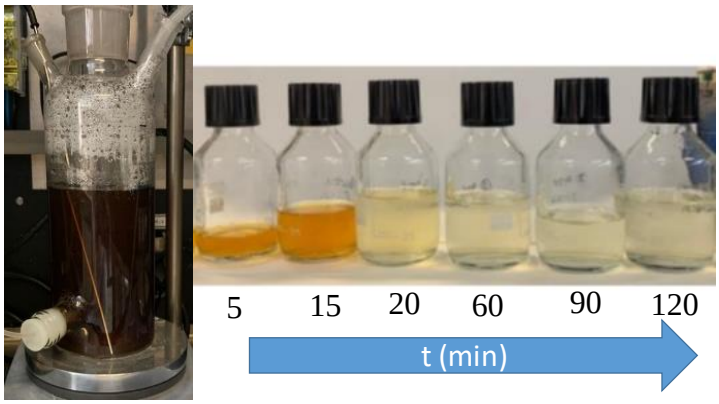

Initial lixiviate

Figure S2. Colour evolution upon the landfill leachate photo-Fenton treatment at 90 ºC ($[TOC]_0$=981 mg/L, $[DQO]_0$=2930 $[H_2O_2]_0$=6200 mg/L, $[Fe^{2+}]_0$ = 10 mg/L, pH_0 = 3)

Declaration of interests

☒ The authors declare that they have no known competing financial interests or personal relationships that could have appeared to influence the work reported in this paper.

☐The authors declare the following financial interests/personal relationships which may be considered as potential competing interests: